IOP PUBLISHING JOURNAL OF GEOPHYSICS AND ENGINEERING

J. Geophys. Eng. **5** (2008) 118–127 doi:10.1088/1742-2132/5/1/012

Frequency extrapolation to enhance the deconvolution of transmitted seismic waves

Saptarshi Dasgupta[1] **and Robert L Nowack**

Department of Earth and Atmos. Sci., 550 Stadium Mall Dr., Purdue University, West Lafayette, IN 47907

E-mail: saptarshi15@gmail.com and nowack@purdue.edu

Received 29 June 2007
Accepted for publication 8 January 2008
Published 14 February 2008
Online at stacks.iop.org/JGE/5/118

Abstract

We investigate the enhanced deconvolution of transmitted seismic waves from distant natural sources using autoregressive extrapolation (AR) and extended time-domain deconvolution. The amplitude spectrum of deconvolved seismograms is often restricted to a reduced frequency range from the use of a water table for the deconvolution. The attenuation effects on the teleseismic seismic waves also reduce the frequency content of the data. We compare the deconvolved spectra obtained from an AR-extended deconvolution (EARD) and an extended time-domain deconvolution (ETDD) technique for teleseismic waves. For EARD, we analyse the spectral content for the deconvolved spectra to differentiate between the domains of known and unknown spectral values. A prediction error filter is used to perform the autoregressive extrapolation to estimate the unknown spectral values. This procedure is applied on 1D and 2D synthetic data to test the approach. The EARD approach is then compared with the ETDD approach which applies an extended high-pass filter to the time-domain deconvolution approach. Both the EARD and ETDD approaches for extending the effective frequency range of the deconvolution results are then compared using observed teleseismic data recorded in southern India.

Keywords: deconvolution, autoregressive extrapolation, receiver functions

Introduction

Deconvolution of transmitted seismic waves from distant natural sources is usually performed using receiver functions where the vertical component is used to deconvolve the horizontal components to identify the P to SV scattered waves (Langston 1979, Owens *et al* 1984). Dasgupta and Nowack (2006) recently used the autocorrelation of the SV component to deconvolve all components of the transmitted 3-component data to remove the source wavelet. Also, Mercier *et al* (2006) used a cross-correlogram technique proposed by Baig *et al* (2005) to estimate the source pulse for the recovery of teleseismic-P Green's function. General overviews of deconvolution techniques for seismic reflection data are given by Webster (1978) and Robinson and Osman (1996). However, these approaches applied to transmitted waves often result in band-limited deconvolutions after filtering and the application of a water table using damped least squares to fill holes in the source spectrum. The attenuation effects on the transmitted seismic waves from distant sources also reduce the frequency bandwidth of the data.

To enhance the resolution of the deconvolved data, we apply an iterative two-stage autoregressive extrapolation (AR) approach to extend the amplitude spectrum of the results from the deconvolution. AR methods have previously been applied to perform high resolution spectral analysis (Kay and Marple 1981). Li and Nowack (2004, 2005) and Nowack and Li (2006) applied AR extrapolation methods for travel-time extrapolation for seismic tomography experiments. The approach was based on the work of Claerbout (1992, 1998),

[1] Current address: Chevron Energy Technology Company, 1500 Louisiana St, Houston TX 77002.

Claerbout and Fomel (2005) and Fomel and Claerbout (2003). In this paper, we apply AR methods to extend the spectra of transmitted seismograms that are band limited resulting from deconvolution. The algorithm attempts to extrapolate the missing frequencies from the known frequencies in the data using a prediction error filter. An earlier approach for extending the deconvolution bandwidth was given by Clayton and Wiggins (1976) using maximum entropy methods and was applied to deconvolved vertical component body waves. More recently, Escalante *et al* (2007) used a sparseness criterion directly in the time domain to enhance the resolution of teleseismic receiver functions. Here we implement the iterative approach for data extrapolation of Claerbout and Fomel (2005) in the frequency domain. This implicitly incorporates a sparseness criterion in the time domain. We then apply this to deconvolved three-component seismic body waves.

A second approach which can be used to extend the frequency range of deconvolved data is an extension of the so-called time-domain deconvolution approach described by Ligorria and Ammon (1999) based on the earlier work of Kikuchi and Kanamori (1982). In this method, a sequence of wavelets is iteratively applied to predict the observed data using an estimated source time function. This results in a series of weighted and delayed pulses which is then band-pass filtered. By increasing the frequency range of the filter, an extended frequency range for the deconvolution can be obtained. In this paper, we will compare the two approaches of extrapolating the missing frequency range of the deconvolution of teleseismic body waves.

Autoregressive methods

Autoregressive extrapolation (AR) can be used to replace missing or corrupted samples with extrapolated estimates of their values. An autoregressive process of order p can be written as

$$y_i = \sum_{k=1}^{p} g_k y_{i-k} + \varepsilon_i = \bar{y}_i + \varepsilon_i, \qquad (1)$$

where g_k are the elements of the optimal predictor, $\bar{y}_i$ is the best linear mean-square predictor of y_i based only on the previous p samples and ε_i is the prediction error. Autoregressive methods can be applied for prediction and extrapolation of data in 1D or higher dimensions (Claerbout and Fomel 2005).

In the two-stage iterative approach to autoregressive extrapolation, the first stage is to find the optimal prediction error (PE) filter from the known data and the second stage is to find the missing data using the resulting PE filter. The output of the PE filter tends to be white and the missing data values are estimated with the same spectrum as the known data. For the case of extrapolation of the amplitude spectrum, this approach is applied in the frequency domain. More details can be found in Claerbout and Fomel (2005) for the iterative extrapolation approach used.

In an early application, Clayton and Wiggins (1976) applied the maximum entropy method (MEM) of Burg (1967) to extend the frequency range of the transmission seismograms after first performing a deconvolution with a water table applied. Lines and Clayton (1977) improved the resolution of vibroseis records by extending the Fourier transform of the impulse response using MEM in designing a prediction error operator.

Walker and Ulrych (1983) estimated models of seismic reflectivity by minimizing an objective function based on constraints of the known frequency domain. They also modified the AR approach of Lines and Clayton (1977) by using the negative frequency band to fill the gap in the frequency band centred at zero frequency. In recent examples, Karsli (2006) combined Wiener filtering and the AR extrapolation approach of Honarvar *et al* (2004) for improving temporal resolution of reflection seismic data. Ulrych and Sacchi (2005) described a number of information-based approaches for inversion as well as extrapolation of geophysical data. Escalante *et al* (2007) applied an explicit sparseness criterion in the time domain to increase the resolution of teleseismic receiver functions. We will follow the iterative extrapolation approach of Claerbout (1992, 1998), Fomel and Claerbout (2003) and Claerbout and Fomel (2005) for the EARD technique. This implicitly incorporates a sparseness criterion in the time domain. We first apply a spectral division with a water table following Clayton and Wiggins (1976) and then apply the iterative AR approach to extend the result (EARD).

Extended time-domain deconvolution

A second approach for the extrapolation in the frequency domain for teleseismic waves is by changing the filter parameters used in the time-domain iterative approach of Ligorria and Ammon (1999). This is a least squares minimization of the difference between the observed seismogram and a predicted signal generated by the convolution of an iteratively updated spike train with the vertical component of the *P*-wave which is often used to estimate the source time function (STF). The STF is cross correlated with the seismogram to estimate the lag of the first and the largest spike in the deconvolution (see also, Kikuchi and Kanamori (1982)). The convolution of the current estimate of the deconvolution is subtracted from the seismogram and this is repeated to estimate other spike lags and amplitudes. By using spikes, the low frequency domain is stabilized in this approach and does not involve other modulating parameters to handle missing frequencies. The final result is obtained by applying a smoothing filter to the result. Although, Ligorria and Ammon (1999) used a Gaussian filter for this, other filters can be applied such as a Butterworth filter and the parameters of this filter can be adjusted to modify the frequency range of the results. Here we will apply a Butterworth filter to smooth the results and to extend the time-domain deconvolution results for transmitted seismic waves from teleseismic sources.

Application to synthetic transmission data

The EARD and ETDD methods described above are first tested using synthetic transmitted waves. For the transmission case, the spikes in figure 1(*a*) represent P-SV scattering from

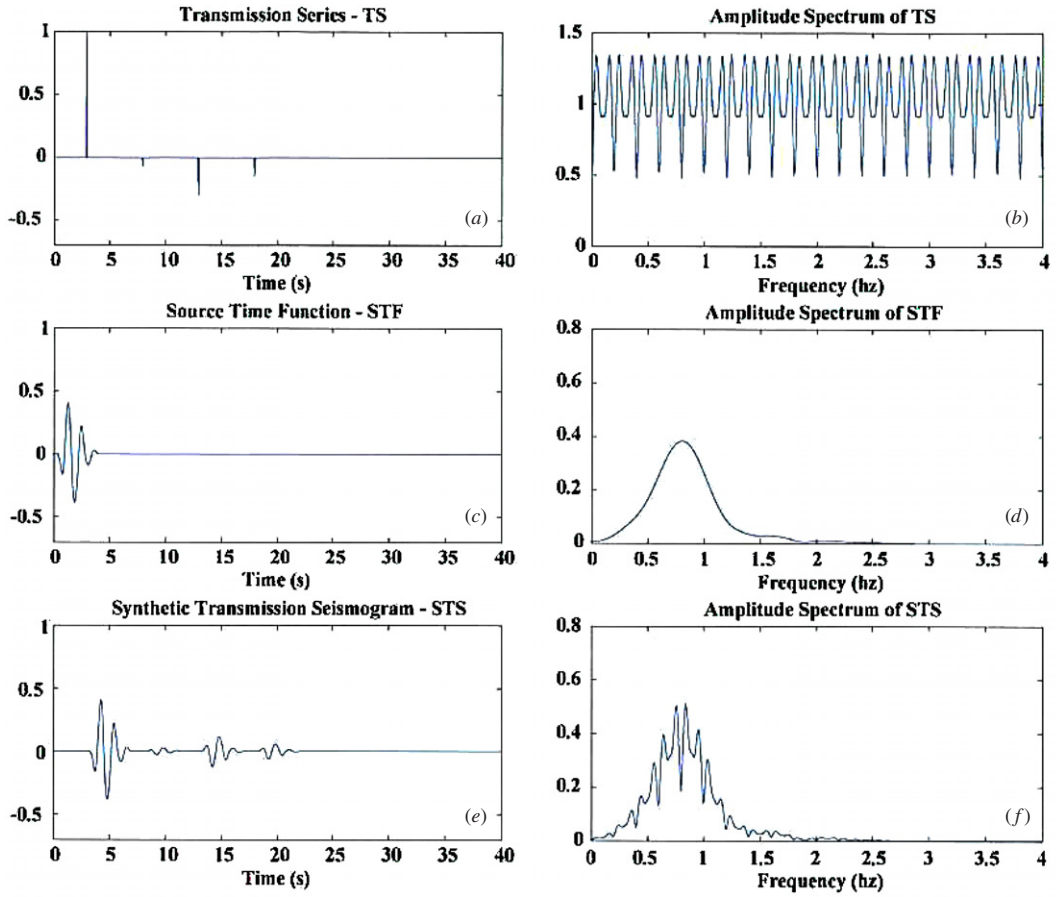

Figure 1. (*a*) The original transmission series with spikes representing sub-surface scatterers. (*b*) The amplitude spectrum of the transmission series in (*a*). (*c*) The source time function recorded from a real seismic event (Tseng and Chen 2006). (*d*) The amplitude spectrum of the source time function in (*c*). (*e*) The synthetic transmission seismogram obtained from the convolution of the transmission series in (*a*) and the source time function in (*c*). (*f*) The amplitude spectrum of the synthetic transmission seismogram in (*e*).

subsurface layers. Figure 1(*b*) shows the amplitude spectrum of the transmission time series in figure 1(*a*). A simple source time function used in this example is from a real seismic event from Tseng and Chen (2006) shown in figure 1(*c*) and its amplitude spectrum is shown in figure 1(*d*). Figure 1(*e*) shows the synthetic transmission seismogram obtained from the convolution of the transmission series in figure 1(*a*) and the source time function in figure 1(*c*). Note the considerable change in the spectrum in figure 1(*f*) as a result of the convolution.

Figure 2 compares the amplitude spectra obtained from the frequency-domain deconvolution (FDD) approach using a water table and the iterative time-domain deconvolution (TDD) technique of Ligorria and Ammon (1999) filtered to the same frequency band using a Butterworth filter. Figure 2(*a*) shows the deconvolved seismogram obtained by deconvolving the synthetic transmission seismogram in figure 1(*e*) with the known source time function in figure 1(*c*) using the FDD approach with a water table and a band-pass filter applied. The amplitude spectrum of the FDD result is shown in figure 2(*b*). Similarly, figure 2(*c*) is the result of deconvolution of the transmission series in figure 1(*e*) and the source time function in figure 1(*c*) using the TDD approach and its amplitude spectrum are shown in figure 2(*d*). In both cases, a zero phase Butterworth filter was applied to restrict the high frequency results. The time-domain results in the two approaches are almost identical, however the TDD better constrains the lower frequencies. The water-table parameter for the FDD approach controls the pattern of the lower frequencies in the FDD technique and is seen to be considerably different in figure 2(*b*) from figure 2(*d*) since in the TDD approach the lower frequencies are incorporated with the addition of the spikes in the iterative process.

Figure 3(*a*) shows the band-limited TDD result which is used to test the autoregressive extrapolation. A symmetric TDD signal is constructed as shown in figure 3(*b*) and then the linear phase shift is removed since our interest is to extrapolate only the amplitude spectrum. After removing the linear phase shift, the spectrum of the zero-phase symmetricized TDD signal is then extrapolated to higher frequencies and finally the linear phase shift is added back to the result to maintain visual consistency. Figure 4(*a*) shows the amplitude spectrum of the zero-phase TDD after removing the linear phase shift from the symmetric signal. Note the repetition of the pattern in the spectrum which helps to extrapolate the pattern to the missing range of frequencies. Also, the spectrum in figure 4(*a*)

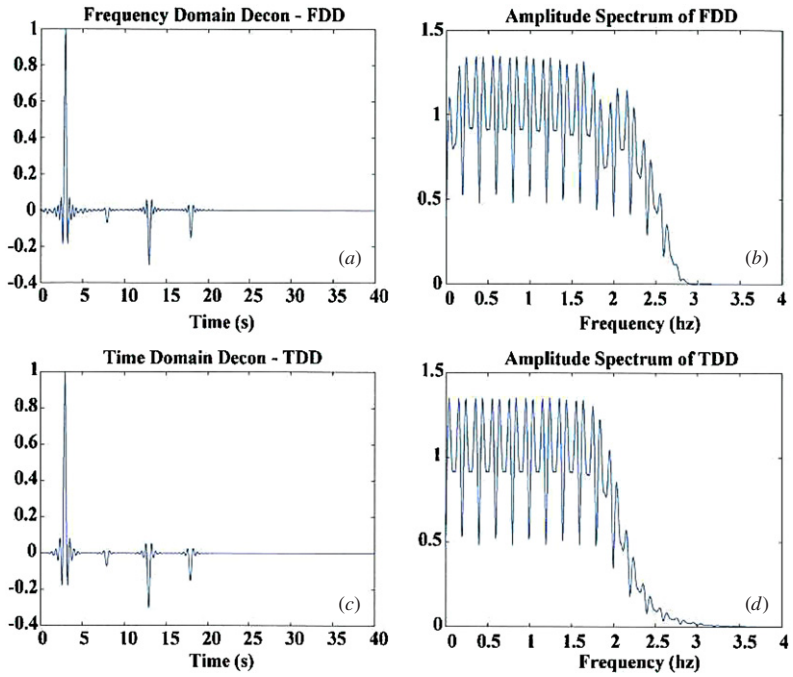

Figure 2. (*a*) Frequency domain deconvolution (FDD) obtained by deconvolving the synthetic transmission seismogram in figure 1(*e*) and STF in figure 1(*c*). (*b*) Amplitude spectrum of FDD in (*a*). (*c*) Time domain deconvolution (TDD) obtained by deconvolving STS in figure 1(*e*) and STF in figure 1(*c*). (*d*) Amplitude spectrum of TDD in (*c*).

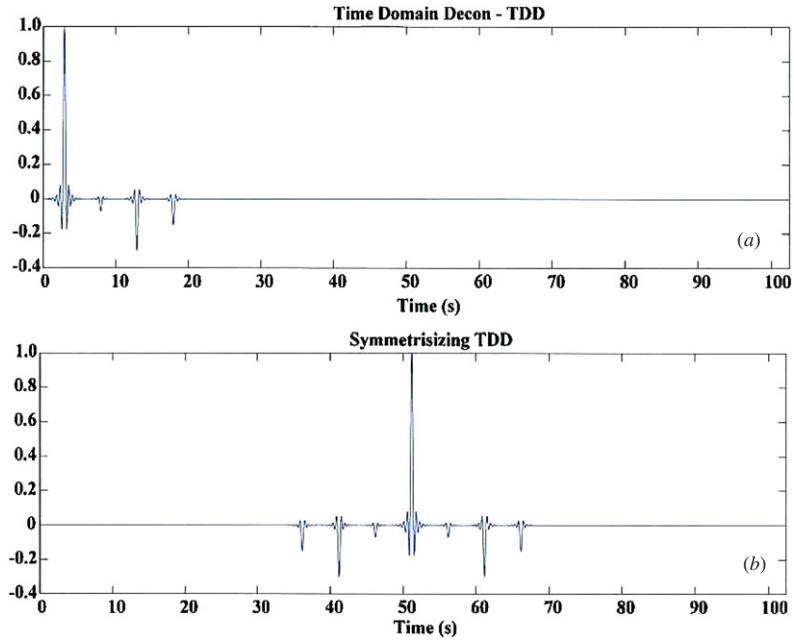

Figure 3. (*a*) The time-domain deconvolution result used to enhance the frequency spectrum by autoregressive extrapolation. It has a band-limited spectrum as seen in figure 2(*b*). (*b*) A symmetric TDD signal is constructed and then the linear phase shift is removed since our interest is to extrapolate only the amplitude spectrum. After removing the linear shift, the spectrum of the zero-phase TDD is then extrapolated and finally the linear shift is added back to the result.

is for the symmetric signal in figure 3(*b*). AR extrapolation is performed on the amplitude spectrum in figure 4(*b*) with the mean removed which is then added back after the extrapolation in figure 4(*c*). The known domain of frequencies is separated from the unknown domain before extrapolation as shown in figure 4(*b*). The number of points defining the known domain needs to be carefully chosen so that it does not interrupt the frequency trend as it has the potential of disrupting the pattern

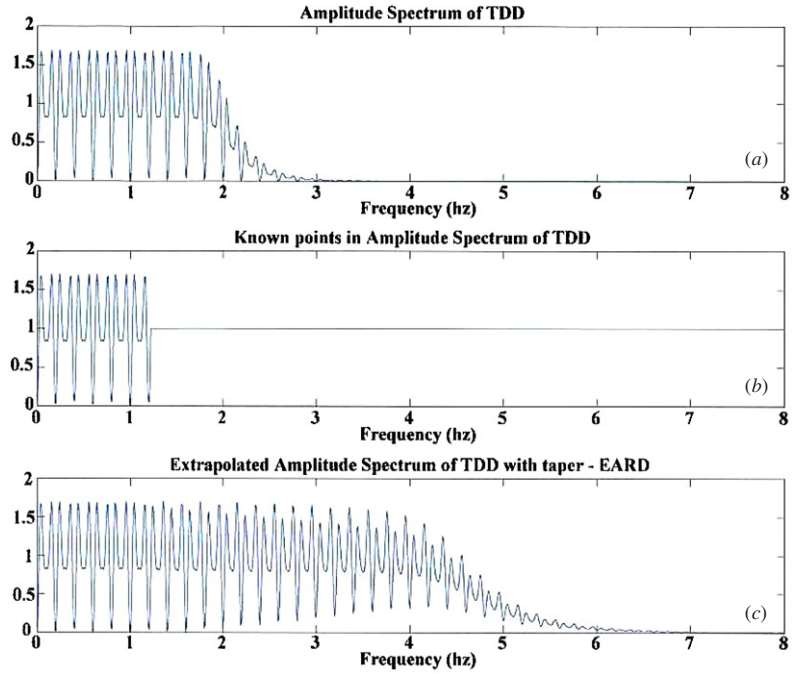

Figure 4. (*a*) The amplitude spectrum of the zero-phase TDD after removing the linear phase shift from the symmetric TDD signal. Note the repetition of the pattern in the spectrum which helps the program to extrapolate the pattern to the missing range of frequencies. (*b*) The domain of the known points in the spectrum is defined which is used to extrapolate the unknown points in the spectrum. In this case, 125 points are considered to be known. The original mean in the spectrum is removed and after extrapolation is added back to the spectrum. (*c*) Extrapolated spectrum with a Butterworth taper added to maintain consistency with the original spectrum in (*a*).

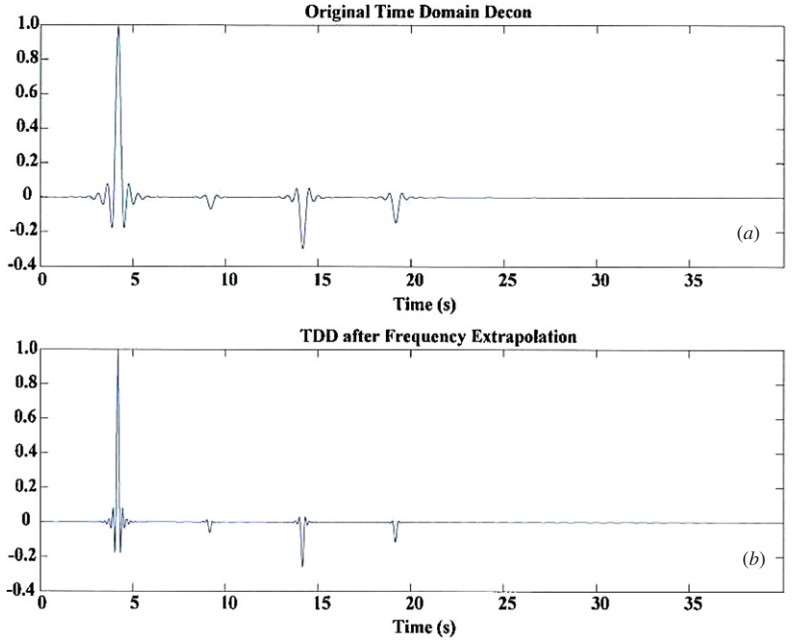

Figure 5. (*a*) The original time-domain deconvolution result with a band-limited spectrum with frequencies up to 2 Hz. (*b*) The time-domain deconvolution signal obtained after AR frequency extrapolation (EARD) up to about 4 Hz. The linear phase previously removed has been added back after frequency extrapolation to maintain consistency.

and then causing erroneous extrapolations. Here several values are used for the selection of the number of frequency domain points and the results with the best extrapolation performance are chosen.

Figure 4(*c*) shows the autoregressive extrapolation result in the frequency domain (EARD) starting with the selected frequencies of the TDD deconvolution result as seen in figure 4(*a*). In this example, 125 frequency samples are

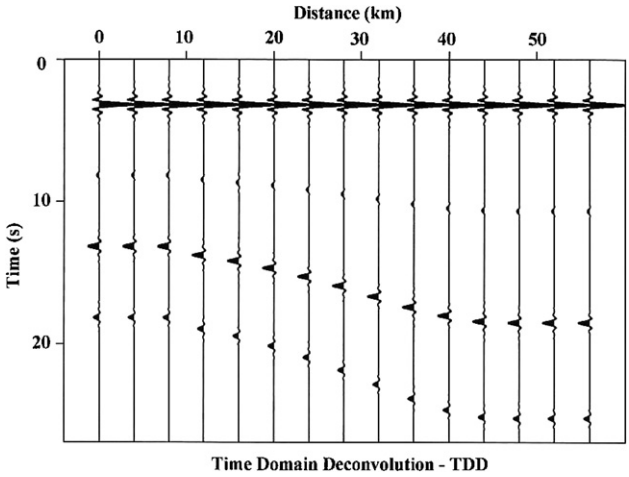

Figure 6. A band-limited time-domain deconvolution (TDD) result for transmitted P-SV waves for a 2D synthetic structure. For transmitted receiver function analysis, the first peak is the direct P that is recorded at the surface followed by other P-SV scattered phases from the crust.

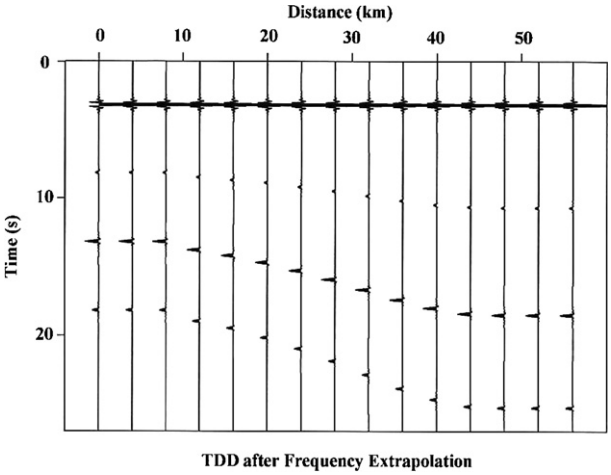

Figure 7. The TDD spectral values are extrapolated to increase the frequency content in the deconvolution (EARD) for each trace in figure 7. Note the considerable improvement in the resolution of the image compared to figure 6 after performing autoregressive frequency (AR) extrapolation.

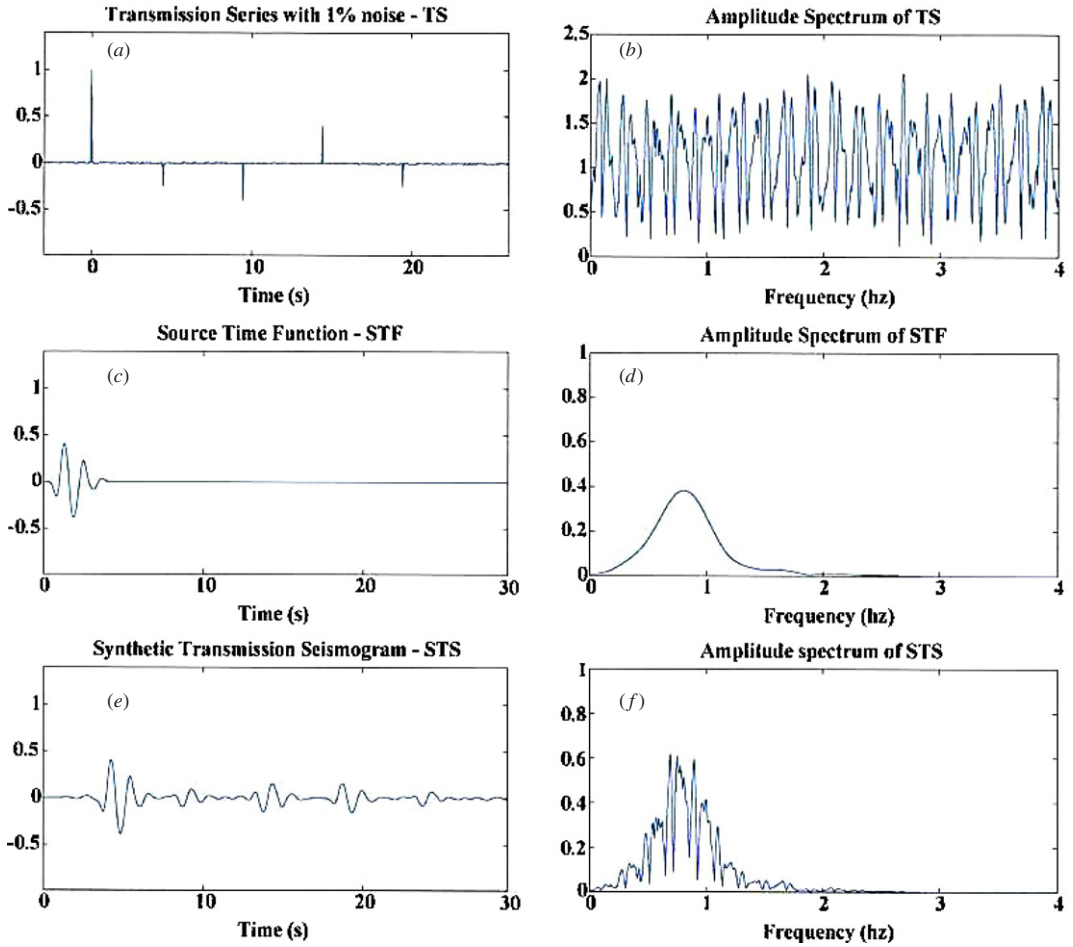

Figure 8. (*a*) The original transmission series with scatterers and noise at 1% of the direct wave amplitude added. (*b*) The amplitude spectrum of the transmission series in (*a*). (*c*) The source time function recorded from a real seismic event (Tseng and Chen 2006) as used in figure 1(*c*). (*d*) The amplitude spectrum of the source time function in (*c*). (*e*) The synthetic transmission seismogram obtained from the convolution of the transmission series in (*a*) and the source time function in (*c*). (*f*) The amplitude spectrum of the synthetic transmission seismogram in (*e*).

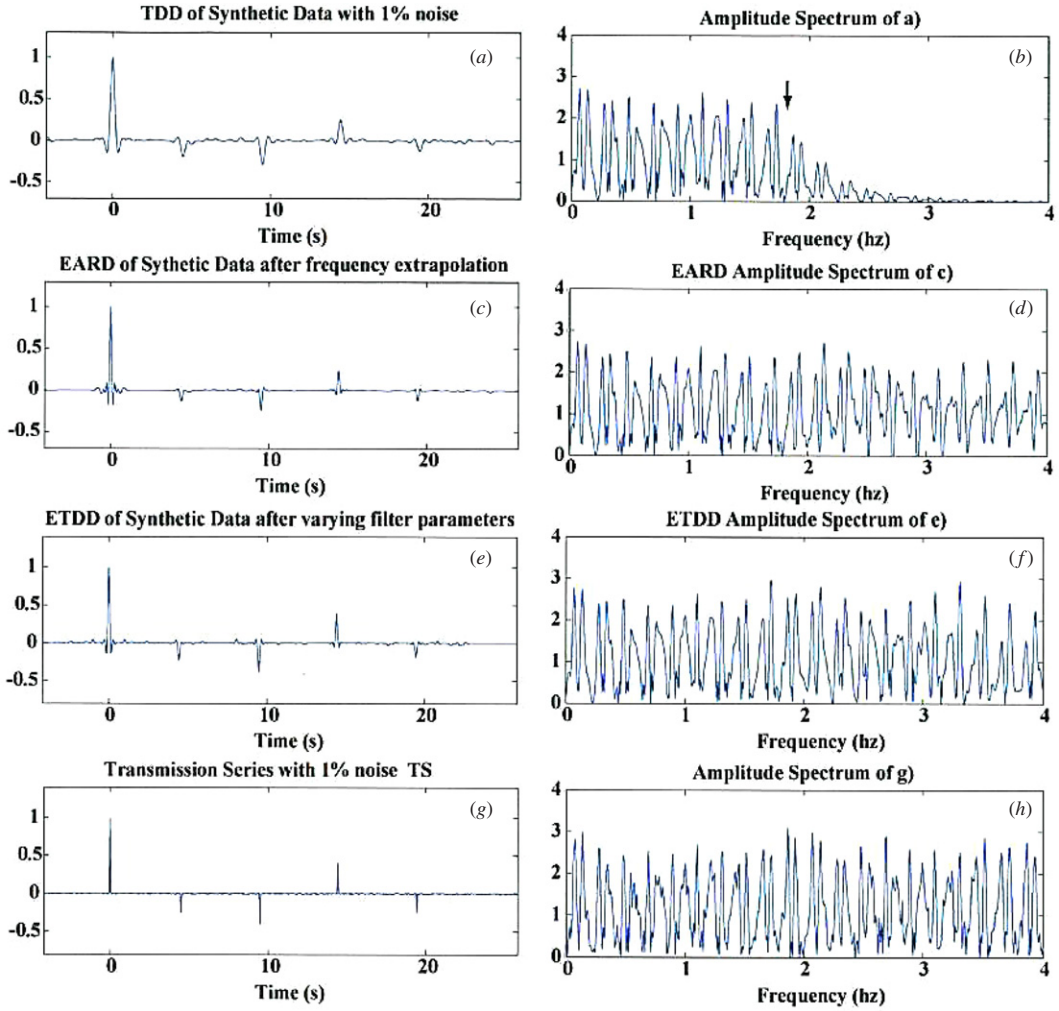

Figure 9. (*a*) Time-domain deconvolution result of synthetic data with noise at 1% of the direct wave amplitude added. (*b*) Band-limited deconvolved amplitude spectrum of (*b*) up to 1.8 Hz—the left side of the arrow is the zone of known points for AR extrapolation. (*c*) Enhanced temporal resolution of EARD result of synthetic data after performing AR extrapolation. (*d*) Band-enhanced amplitude spectrum of (*c*) after AR extrapolation to 4 Hz. (*e*) Enhanced temporal resolution of the TDD result of synthetic data after increasing the corner frequency of the filter in the modified TDD approach—ETDD. (*f*) Band-enhanced amplitude spectrum to 4 Hz of (*e*) altering filter parameters. (*g*) Original transmission series with noise at 1% of the direct wave amplitude added. (*h*) Amplitude spectrum of (*g*).

considered to be in the known domain. The extrapolation for the unknown points in the spectrum was performed with a prediction error filter (PEF) of length 55 points. The length of the PEF is a hyper-parameter that can be selected based on the Akaike information criterion and is discussed by Ulrych and Sacchi (2005). Here we use a more empirical approach of using a range of values and selecting the one with the best extrapolation results.

The original mean in the spectrum that was removed earlier is added back to the extrapolated spectrum at this stage. Also, a low-pass Butterworth filter is applied to maintain consistency of the pattern between the original spectrum in figure 4(*a*) and the extrapolated spectrum in figure 4(*c*). A comparison of the original TDD deconvolution result with the frequency-extrapolated EARD is shown in figure 5. Initially the TDD result has a restricted spectrum with frequencies up to 2 Hz as seen in figure 5(*a*). After extrapolation, the TDD signal had an enhanced frequency range up to 4 Hz with an increased temporal resolution as seen in figure 5(*b*). The linear phase previously removed prior to extrapolation has been added back for consistency.

We performed a second test of the EARD method using transmitted synthetics shown in figure 6 for a deepening basin structure, which shows a band-limited time-domain deconvolution result. For transmitted receiver function analysis, the first peak would correspond to the direct P-wave that is recorded at the surface followed by P-SV scattered phases from the crust. The spectral values are extrapolated to increase the frequency content of the band-limited spectrum of the traces in figure 6 using AR extrapolation (EARD) as described previously. Note the considerable improvement in the temporal resolution of the image in figure 7 compared to that in figure 6.

Before applying extrapolation techniques to observed teleseismic events, we apply both the EARD and ETDD

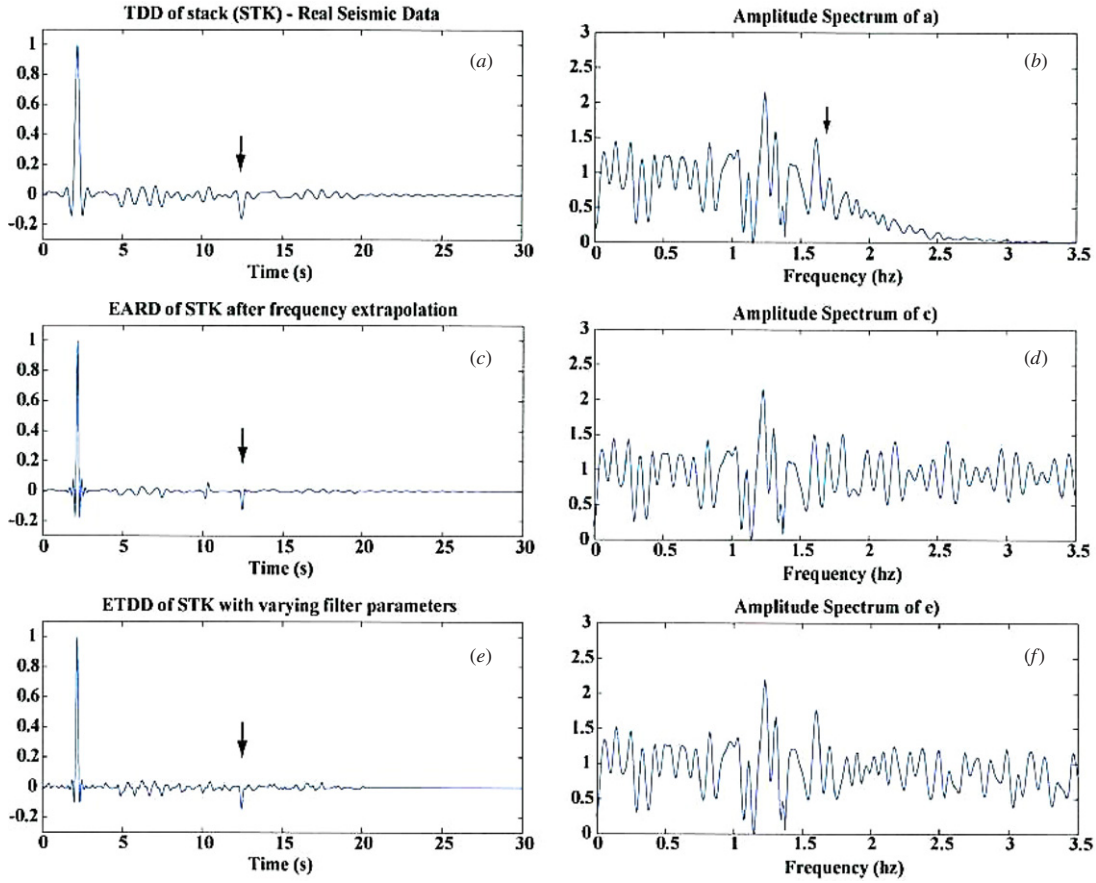

Figure 10. (*a*) Deconvolved P-waves of stacked channels from array GBA using TDD where the arrow indicates the PpPmp phase reflected from the Moho. (*b*) Band-limited amplitude spectrum up to 1.6 Hz for (*a*)—the left side of the arrow is taken as the zone of known points for AR extrapolation. (*c*) Enhanced temporal resolution after performing EARD extrapolation to 3.5 Hz. (*d*) Band-enhanced EARD amplitude spectrum after AR extrapolation to 3.5 Hz. (*e*) Enhanced temporal resolution by extending the filter parameters in the TDD approach—ETDD. (*f*) Band-enhanced ETDD amplitude spectrum for (*e*).

approaches to 1D synthetics with noise added. Figure 8(*a*) shows the transmission time series with noise at 1% of the direct wave amplitude added. However, the level of noise is on the order of 5% of the smallest scattered wave amplitudes. The resulting spectrum is shown in figure 8(*b*). Figures 8(*c*) and (*d*) show the same source time function and its amplitude spectrum respectively from figure 1 used for this test. The convolution of the transmission time series in figure 8(*a*) and the source time function in figure 8(*c*) are shown in figure 8(*e*) with its amplitude spectrum in figure 8(*f*).

Figure 9(*a*) shows the time-domain deconvolution (TDD) result of synthetic data with added noise in the transmission series. The amplitude spectrum is the band-limited deconvolved spectrum shown in figure 9(*b*) from the symmetricized signal. The left side of the arrow is considered the zone of the known spectrum and the right side is the unknown spectrum zone which will be filled in by using the AR technique described earlier. The time-domain result of the AR extrapolation is shown in figure 9(*c*) where the spikes indicate the higher frequencies that have been incorporated and figure 9(*d*) shows the enhanced amplitude spectrum.

By increasing the corner frequency of the Butterworth filter in the time-domain deconvolution of Ligorria and Ammon (1999) (ETDD), higher frequencies of interest can be attained from the original TDD results. Thus, frequency extrapolation can also be performed by varying filter parameters after obtaining the TDD deconvolved result. The time-domain result obtained using a corner frequency of 4 Hz is shown in figure 9(*e*) and has all the spikes with some noticeable smaller artefacts generated due to the presence of noise in the time series. The enhanced spectrum of figure 9(*e*) is shown in figure 9(*f*). For comparison, the original time series with noise at 1% of the direct wave amplitude added is shown in figure 9(*g*) with its amplitude spectrum in figure 9(*h*) for the symmetricized signal. From these results, AR extrapolation (EARD) appears to emphasize only the original spikes in the results as compared to the ETDD results where smaller peaks are also being incorporated. This results from the fact that the TDD approach is an iterative one in which for a complicated observed data, a large number of spikes can be included in the deconvolved time series. Also, the EARD has an implicit sparseness constraint incorporated in the frequency extrapolation. Although, the extended results are similar, they both slightly differ from the actual spectrum. Nonetheless, good pulse compression can be seen for both results.

Application to observed teleseismic data

The EARD and ETDD techniques described above are applied to observed teleseismic events recorded in the Gauribidanur Array (GBA) from southern India. Deconvolved P-waves were studied by Tseng and Chen (2006) to understand the geometry of the Moho from reflected PpPmp phases. Figure 10(*a*) shows the deconvolved P-wave of stacked channels from station GBA where the PpPmp phase reflected from the Moho is about 10 s after the direct P phase in the trace shown by the arrow. The band-limited amplitude spectrum of the receiver function is shown in figure 10(*b*) where the frequencies are limited up to 1.5 Hz. The left side of the arrow is taken as the known spectrum which is used for the autoregressive extrapolation. Figure 10(*c*) shows the EARD result of the enhancement of the temporal resolution using autoregressive extrapolation. The EARD extrapolated spectrum up to 3.5 Hz is shown in figure 10(*d*). It is interesting to note that in the AR approach for extrapolations, the critical peak at 10 s for the PpPmp phase is distinctly recovered with the higher frequencies. The time-domain result of the frequency enhancement by extending the corner frequency of the filter (ETDD) is shown in figure 10(*e*). The ETDD extrapolated spectrum of figure 10(*e*) is shown in figure 10(*f*). A direct comparison of the EARD extrapolation and the ETDD extension indicates that the noise associated with the trace also gets enhanced in the ETDD result which is more subdued in the AR extrapolation. This results from the implicit sparseness constraint in the EARD approach and is similar to that observed in the synthetic test performed in figure 9.

Conclusions

The EARD and ETDD approaches were investigated to extrapolate spectra of transmission seismograms from distant teleseismic events. The EARD technique was first used to extrapolate frequencies for 1D synthetics and the method was found to be feasible to effectively fill in and extend missing spectral values. We performed a second test with this method to enhance the temporal resolution from a deepening basin structure. An alternative approach of extending the frequency results (ETDD) uses a variable band-pass filter to extend the deconvolution results by increasing the corner frequency of the Butterworth filter which modifies the time-domain deconvolution approach of Ligorria and Ammon (1999). We compared the results of the EARD and ETDD frequency extrapolations using 1D synthetics with added noise. A test was then performed using observed teleseismic data from an array in India where a Moho-reflected phase PpPmp was enhanced by filling missing spectral values with the EARD and ETDD techniques. The results obtained from tests on synthetic and observed data indicated that the EARD extrapolation identified the larger peaks in the time series, whereas the ETDD approach also enhances the small noise components along with the larger peaks in the data thus generating some small artefacts. This results from the implicit sparseness constraint in the EARD approach. Nonetheless, for both methods, the larger peaks were well enhanced. However, the ETDD approach has the advantage of simplicity of implementation over the EARD approach.

Acknowledgments

We thank Blacknest of the Atomic Weapons Establishment (AWE), United Kingdom, for originally providing the data. We also thank Tai-Lin Tseng and Wang-Ping Chen for helpful discussions on the data which were also used in their earlier paper. We also thank the reviewers for their constructive comments.

References

Baig A M, Bostock M G and Mercier J-P 2005 Spectral reconstruction of teleseismic P Green's functions *J. Geophys. Res.* **110** B08306

Burg J P 1967 Maximum entropy spectral analysis *37th Annual International SEG Meeting (Oklahoma City)*

Claerbout J F 1992 *Earth Soundings Analysis: Processing versus Inversion* (Cambridge, MA: Blackwell Scientific Publications)

Claerbout J F 1998 Multidimensional recursive filters via a helix *Geophysics* **63** 1532–41

Claerbout J F and Fomel S 2005 Geophysical Estimation by Example: Geophysical Soundings Image Construction: Multidimensional Autoregression, web book, http://sepwww.stanford.edu/sep/prof/index.html

Clayton R W and Wiggins R A 1976 Source shape estimation and deconvolution of teleseismic body waves *Geophys. J. R. Astron. Soc.* **47** 151–77

Dasgupta S and Nowack R L 2006 Deconvolution of three-component teleseismic P-waves using the autocorrelation of the P to SV scattered waves *Bull. Seism. Soc. Am.* **96** 1827–5

Escalante C, Gu Y J and Sacchi M 2007 Simultaneous iterative time-domain sparse deconvolution to teleseismic receiver functions *Geophys. J. Int.* **171** 316–25

Fomel S and Claerbout J F 2003 Multidimensional recursive filter preconditioning in geophysical estimation problems *Geophysics* **68** 577–88

Honarvar F, Sheikhzadeh H, Moles M and Sinclair A N 2004 Improving the time-resolution and signal-to-noise ratio of ultrasonic NDE signals *Ultransonics* **41** 755–63

Karsli H 2006 Further improvement of temporal resolution of seismic data by autoregressive (AR) spectral extrapolation *J. Appl. Geophys.* **59** 324–36

Kikuchi M and Kanamori H 1982 Inversion of complex body waves *Bull. Seism. Soc. Am* **72** 491–506

Langston C A 1979 Structure under Mount Rainier, Washington, inferred from teleseismic body waves *J. Geophys. Res.* **84** 4749–62

Li C and Nowack R L 2004 Application of autoregressive extrapolation to seismic tomography *Bull. Seism. Soc. Am.* **94** 1456–66

Li C and Nowack R L 2005 Seismic tomography using travel-time surfaces for experiments in the laboratory *J. Geophys. Eng.* **2** 231–7

Ligorria J P and Ammon C J 1999 Iterative deconvolution and receiver-function estimation *Bull. Seism. Soc. Am.* **89** 1395–400

Lines L R and Clayton R W 1977 A new approach to vibroseis deconvolution *Geophys. Prospect.* **25** 417–33

Kay S M and Marple S L 1981 Spectrum analysis—a modern perspective *Proc. IEEE* **69** 1380–419

Mercier J-P, Bostock M G and Baig A M 2006 Improved Green's functions for passive-source structural studies *Geophysics* **71** SI95–SI102

Nowack R L and Li C 2006 Application of autoregressive extrapolation to the cross-borehole geometry *Studia Geophysica Geodaetica* **50** 337–48

Owens T J, Zandt G and Taylor S R 1984 Seismic evidence for an ancient rift beneath the Cumberland Plateau, Tennessee: a detailed analysis of broadband teleseismic P-waveforms *J. Geophys. Res.* **89** 7783–95

Robinson E A and Osman O M 1996 *Deconvolution 2* (Tulsa, OK: SEG) *Geophysics Reprint Series* vol 17)

Tseng T-L and Chen W-P 2006 Probing the Southern Indian shield with *P*-wave receiver-function profiles *Bull. Seism. Soc. Am.* **96** 328–33

Ulrych T J and Sacchi M D 2005 *Information-Based Inversion and Processing with Applications* (Amsterdam: Elsevier)

Walker C and Ulrych T J 1983 Autoregressive recovery of the acoustic impedance *Geophysics* **48** 1338–50

Webster G M 1978 *Deconvolution* (Tulsa, OK: SEG) Geophysics Reprint Series